Modeling and Real-time Scheduling of Large-Scale Batteries for Maximizing Performance

Eugene Kim and Kang G. Shin
Department of Electrical Engineering and Computer Science
The University of Michigan – Ann Arbor, U.S.A.
{kimsun,kgshin}@umich.edu

Jinkyu Lee
Department of Computer Science and Engineering
Sungkyunkwan University (SKKU), Republic of Korea
jinkyu.lee@skku.edu

***Abstract*—Modern electric vehicles are equipped with an advanced battery management system, responsible for providing the necessary power efficiently from batteries to electric motors while maintaining the batteries within an operational region. Because the discharge-rate and temperature affect battery health and efficiency significantly, batteries should be managed to mitigate their discharge and thermal stresses.**

In this paper, we develop a real-time, efficient integrated system for managing the discharge-rate and temperature of batteries. To achieve this objective, we first construct a prognosis system predicting the likely states of batteries' capacity and capability. Based on the prognostic estimation of the impact of the temperature and discharge-rate on the performance, we solve an optimization problem to search for efficient discharging and cooling scheduling. Our experimentation and simulation results demonstrate that the proposed management enhances system performance up to 85.3%.

I. Introduction

Electric vehicles (EVs) powered by batteries are the key in reducing global warming and rising fuel cost. However, they have not fully replaced internal combustion engine vehicles due mainly to their high price resulting from the high battery cost and a risk of explosion under extreme conditions. For instance, Tesla Motors plans to invest 2 billion dollars within next three years to produce cheaper batteries for EVs via mass production [1]. An effective battery management system (BMS) is a must in addressing the challenges of EVs; efficient charging/discharging can reduce the required number of battery cells and the charging frequency [2–4]; thermal management improves battery's capacity while protecting batteries from fast performance degradation and explosion [5–7].

The methods of controlling discharge-rate and temperature are considered for deployment in EVs, since they are known to improve the battery capacity and lifetime. However, there are several obstacles to overcome in order to optimize and deploy solutions in real vehicles. First, an accurate estimation of battery behavior related to the battery performance and its degradation is very complicated. While the battery behavior varies non-linearly with temperature and the required discharge-rate, their prediction requires the understanding of entire battery electrochemical processes. This difficulty of accurate prediction makes it harder to choose/control the discharge-rate and temperature of batteries. Moreover, the behavior and performance of batteries in a pack are not homogeneous; battery packs' performance and behavior are not expected to be the same even during the manufacturing stage. Enhancing one aspect of the performance (e.g., battery lifetime) may also affect the other aspect (e.g., capacity). For example, battery capacity improves temporarily at "instant high temperature" due to the increased chemical reaction rate and ion mobility. However, the "cumulative exposure to high temperature" causes the permanent lifetime to decline because of its acceleration of irreversible side reaction. Also, we should consider the timely scheduling of charge/discharge as well as thermal control, because batteries would otherwise be overheated or over charged, potentially leading to catastrophic accidents. This requires determination of deadlines to protect the batteries from significant loss of performance and/or reliability. These obstacles call for an integrated *cyber-physical system* (CPS) in which batteries and energy management devices are physical components. We should thus take all the entities into account, and achieve effective and timely control to improve battery performance based on physical properties of the system components.

To this end, this paper proposes a prognosis scheme and a real-time scheduling algorithm for controlling the discharge/charge current and temperature to extend battery *operation-time* within its warranty period. The operation-time is defined as the "cumulative time for batteries to provide the required power after a full charge" [2]; with a longer operation time, we can drive farther or longer with the same amount of energy. Note that battery capacity monotonically decreases over time, because the performance of a battery degrades over time. Therefore, the battery capacity at any time during the warranty period is at least as much as that at the end of warranty period. That is, an efficient BMS must provide the required power for an extended operation time even at the end of warranty period.

To control the battery discharge/charge current and temperature efficiently to maximize battery operation-time, we must first characterize the impact of discharge/charge current and temperature on battery behaviors that affect battery operation time and its degradation. To construct an accurate battery behavior model for prognosis, we use two regression schemes: symbolic regression for a generic form of battery behaviors model and linear regression for tuning the generic model to each battery pack. Based on the behavior model, we can then schedule the discharge/charge and temperature of batteries to maximize operation-time (t_o) within the warranty period. An analysis of the optimal solution allows us to derive an efficient real-time scheduling policy for controlling discharge-rate and cooling of batteries so as to achieve our goal.

1052-8725/15 $31.00 © 2015 IEEE
DOI 10.1109/RTSS.2015.11

The main contributions of this paper are to:

- develop a prognosis system that constructs the model form and its coefficients using *symbolic regression*, which is the first attempt of applying the symbolic regression to battery modeling;
- design a real-time scheduling framework to determine both battery discharge/charge rate and temperature to maximize battery operation-time during the warranty period based on the model construction; and
- demonstrate the efficiency of the proposed system via an in-depth, realistic evaluation.

The paper is organized as follows. Section II provides the background of battery performance and our target BMS architecture. Section III formally states the problem from a cyber-physical perspective. Section IV describes how we construct battery behavior models for predicting batteries' future states, and Section V details how to schedule discharge/charge current and battery temperature for improving battery performance based on the battery behavior models. Section VI evaluates the proposed battery behavior prediction using our behavior models, and performance optimization. Finally, the paper concludes with Section VII.

II. Target BMS Architecture

This section introduces our target BMS architecture for EVs. We first describe the requirements of a good BMS for electric vehicles as shown in Fig. 1, and then our target BMS architecture.

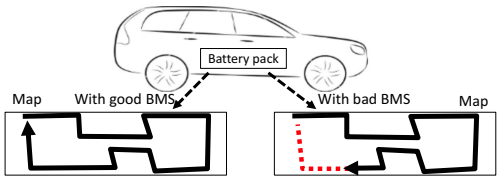

Fig. 1. A good BMS allows electric vehicles (EVs) to drive longer distance and time (longer operation-time) for given batteries.

A. What is a good BMS?

A battery pack in EVs supplies DC power to an inverter which operates the electric motors in EVs. To operate motors, a power inverter needs an applicable input voltage during the vehicle's operation. Therefore, a good BMS enables drivers to use their vehicles for a long operation-time by maintaining the output voltage no less than the applicable motor input voltage as shown in Fig. 1. The operation-time should also be kept long enough during the battery warranty period; otherwise, the vehicle requires a larger battery pack and/or more batteries must be recharged more frequently. Therefore, we must consider battery degradation to meet the specified warranty.

However, current battery systems still cannot achieve the required performance and replace the internal combustion engines mainly because they do not utilize batteries' full capacity and capability in real vehicle applications. The power requirement of an EV is high and changes abruptly [8–10], because drivers frequently accelerate/decelerate their vehicles that weigh at least one ton during driving. It can also cause inefficiency and/or damage to battery, potentially leading to large energy losses and fast voltage drop within the warranty period. Therefore, a battery management system (BMS) in an EV is responsible for providing motors with the required power while protecting the battery cells from damage, excessive energy loss and life reduction caused by short bursts of power transfer. To achieve such functions, a BMS is often comprised of (i) a large number of battery cells that can supply the high current (hundreds of amperes) with the high output voltage (tens or hundreds of volts), and (ii) an auxiliary system to mitigate thermal and discharge stresses.

B. Target BMS architecture

We consider a BMS architecture which consists of a *regenerative braking system* (Section II-B1), a *discharge-rate management system* (Section II-B2), and a *thermal management system* (Section II-B3) as shown in Fig. 2. Although the architecture is relatively simple, it is equipped with essential functions and structures for efficient battery management, and each component is widely studied in battery and automotive industries. It allows batteries to save energy generated from a braking system, mitigate the discharge/charge stress via an energy buffer, and regulate the thermal condition for the efficient battery operation, which are detailed next.

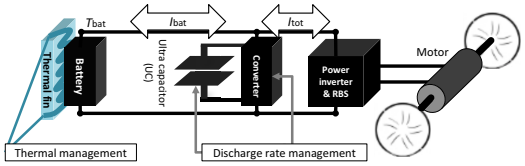

Fig. 2. A target battery management architecture for EVs: a regenerative braking system (RBS) enables a battery system to store dissipated energy from the braking system, and discharge-rate and thermal management reduce energy loss while mitigating the stress of batteries.

1) Regenerative braking system (RBS): To reuse the energy dissipated in their braking system, most EVs are equipped with a regenerative breaking system (RBS) in order to increase operation-time. During braking, the RBS converts the vehicle's kinetic energy into electrical energy that can be stored in batteries for reuse to power the vehicle. Its effectiveness has been substantiated in terms of fuel economy [11–13]. Although the RBS improves the utilization of energy, the high recharging current for a very short period of time has a negative impact on the battery's health. Therefore, researchers introduced an auxiliary system as described next.

2) Discharge-rate management: Battery health and performance are damaged by short bursts of discharging current supplied to motors and recharging current generated from the RBS. To remedy this problem, researchers proposed deployment of ultra-capacitors (UCs); a BMS equipped with UCs and batteries is called a *hybrid energy storage system* (HESS). In a HESS, UCs are used as an energy buffer to smooth rapid power fluctuations in and out of the battery of an EV [3, 14–16]. Therefore, a HESS enables batteries to supply the average power required for operating vehicles, while UCs provide the sudden power surges required for acceleration and also accommodate instantaneous regenerative energy from the RBS.

3) Thermal management: Along with discharge-rate management, thermal management is one of the most important factors for a reliable BMS, and existing BMSes have thus employed thermal management policies so as to prevent battery cells from very high and low temperatures which may likely cause explosion and malfunction, respectively. Basically, the BMS monitors the temperature of battery cells, and triggers the thermal control when the temperature deviates from the normal operational range through "thermal fins", "air cooling system", or "liquid coolant system" [6, 7, 17, 18]. This control includes both cooling and heating, and existing controls are all or nothing, i.e., they cool/heat all the battery cells connected in parallel. Active fine-grained thermal control has also been proposed to reduce the safety margin, and then enhance the system performance based on its thermo-physical characteristics [5]. In principle, we increase the battery temperature for accelerating its chemical reaction if a large amount of power is required, and decrease the temperature when the battery needs to rest.

III. Problem Formulation and Solution

Thus far, we have discussed the requirements of a good BMS and our target BMS architecture meeting the requirements. To develop a good BMS, we should extend operation-time during the warranty period by maintaining both discharge-rate and temperature of battery within an efficient operational range. Presented below are a formal statement of our BMS problem and and an overview of our solution approach.

A. Problem statement

We have already introduced the target BMS architecture that can regulate battery temperature and discharge-rate for efficient use of batteries. Specifically, the architecture regulates the temperature and discharge rate during every time interval, as described in Fig. 2 and the following matrix:

$$X = \begin{pmatrix} (I_{\text{bat}}, T_{\text{bat}})^{11} & \dots & (I_{\text{bat}}, T_{\text{bat}})^{1n} \\ \dots & \dots & \dots \\ (I_{\text{bat}}, T_{\text{bat}})^{m1} & \dots & (I_{\text{bat}}, T_{\text{bat}})^{mn} \end{pmatrix},$$

where $(I_{\text{bat}}, T_{\text{bat}})^{ij}$ are the battery discharge current and temperature during the j^{th} time interval of cycle i. A row vector consists of inputs $(I_{\text{bat}}, T_{\text{bat}})$ at every time interval from the start to the end of the battery operation (consisting of n intervals) in a cycle. Note that a charge/discharge cycle is defined as the process of fully charging a rechargeable battery and discharging it to a load. We need m input vectors for every cycle in the warranty period (consisting of m cycles). Therefore, battery temperature and discharge rate are the control knobs that can be scheduled at every time interval to improve the system performance in EVs as seen in Fig. 3. For instance, if we scheduled to store much energy into UCs from batteries and an RBS when the vehicle decelerates, we can supply more power when it accelerates while maintaining the battery discharge rate within an efficient operational range. Our goal is to maximize system performance by making the battery supply the required power to EV as long as possible by selecting the control knob matrix X. To evaluate the system performance, we introduced the operation-time (t_{o}) which measures how long the battery provides the EV the required power ($P_{\text{req}}(t)$). To increase the operation-time of battery, we should maintain

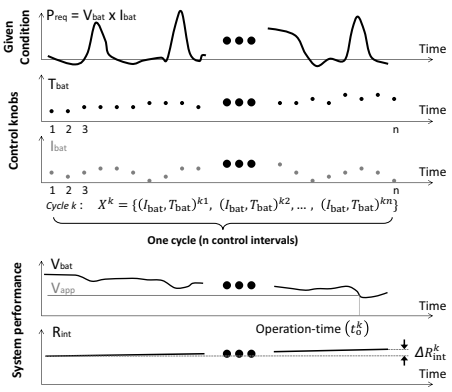

Fig. 3. An example of discharge current (I_{bat}) and temperature (T_{bat}) controls under a given power requirement ($P_{\text{req}}(t)$)

battery output voltage (V_{o}) above the applicable voltage (V_{app}) of motors as long as possible because it is the minimum required voltage for operating electric motors as shown in the last graph of Fig. 3. We also study the performance degradation of a battery, since it affects the operation-time (t_{o}) at later cycles in the warranty period. We measure an internal resistance (R_{int}) at the first interval of each cycle to see the changes in the degradation. Note that the degradation depends on how the battery is used in previous cycles. Therefore, we should consider how battery degradation would change due to the control knob matrix X. Fig. 3 shows an example of their discharge-rate and temperature control over time (control interval) within a cycle for the given power requirement. The operation-time ends when the output voltage of battery reaches a certain pre-determined voltage value (which is dependent on the motors in EVs). During the cycle, battery degrades by ΔR_{int}.

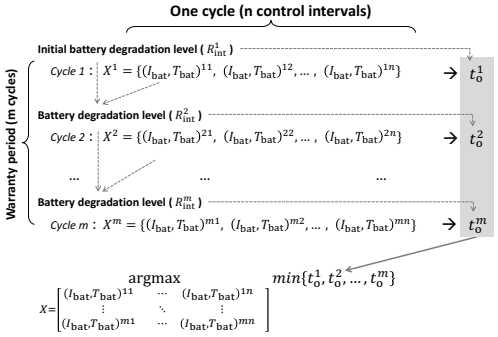

Fig. 4. The k^{th} row of the control knob matrix X and the battery degradation level (R^k_{int}) at the k^{th} cycle affect battery operation-time at the k^{th} cycle. Our purpose is to find the control knob matrix X that maximizes the minimum operation-time.

With the above system model, assumptions and notations, Fig. 4 depicts our problem, which can be formally stated as:

Given power requirement $\{P_{\text{req}}(t)\}_{0<t<t_{\text{max}}}$, n maximum control intervals, m warranty cycles, battery temperature upper bound (T_{ub}) and lower bound (T_{lb}), and battery discharge current upper bound (I_{ub}) and lower bound (I_{lb}),

determine the control knob matrix X consisting of scheduling vectors $X^i = \{(I_{\text{bat}}, T_{\text{bat}})^{i1}, \dots, (I_{\text{bat}}, T_{\text{bat}})^{in}\}$ of battery

discharge current (I_{bat}^{ij}) and temperature (T_{bat}^{ij}) at each control interval $j \in \{1, \ldots, n\}$ for each cycle $i \in \{1, \ldots, m\}$ so as to maximize the minimum operation-time $min\{t_{\text{o}}^1, \ldots, t_{\text{o}}^m\}$ within the warranty cycles (m). The objective function of this optimization can then be defined as

$$\begin{aligned} \underset{\text{X}}{\text{argmax}} \quad & min\{t_{\text{o}}^1, \ldots, t_{\text{o}}^m\}, \\ \text{subject to} \quad & T_{\text{lb}} < T_{\text{bat}}^{ij} < T_{\text{ub}}, \\ & I_{\text{lb}} < I_{\text{bat}}^{ij} < I_{\text{ub}}. \end{aligned}$$

The reason for our focus on the minimum operation-time is that we want to maximize the EV's drivability during the entire warranty period. By finding the minimum operation-time, we can guarantee that the BMS is able to supply energy for the operation-time at any cycle within the warranty period. We also assume that the degradation in a cycle does not affect the operation-time in that cycle to simplify the problem. This assumption is reasonable because battery degrades very slowly and its change has a negligible influence on battery capacity within a cycle as seen in the supplementary file [19]. This assumption allows us to consider the control knob's impact on the operation-time and battery degradation separately.

We exploit both discharge-rate and thermal management to prevent the battery from a large voltage drop caused by high required current. By pre-charging UCs and transferring charges when the battery is required to supply large current, discharge-rate management can relieve the battery from discharge stresses while providing the required current to the electric load. Also, we can increase battery output voltage temporarily by increasing battery temperature, because it decreases battery internal resistance [5]. Boosting the output voltage via the discharge current and thermal management requires power, which may reduce the available energy from the battery for future usage. That is, we have to maintain battery output voltage while consuming the least amount of energy (E_{total}), since the output voltage is approximately proportional to the amount of the remaining energy in the battery. Therefore, to efficiently maintain battery output voltage, we have to consider the energy consumption as well.

B. Solution Approach from a CPS Perspective

Battery management requires understanding of chemical reactions since generating electricity entails complex chemical processes related to various physical conditions. Battery output voltage is also affected by the physical conditions such as battery temperature and discharge-rate. Therefore, we should figure out the relationship between the output voltage and controllable physical conditions (control knobs). However, it is difficult to understand the electrochemical processes to capture the relationship between them. Also, each type of a battery has its own chemical reaction mechanism that generates energy. To make matters worse, battery behaviors and its performance are not the same even for the same type of batteries. To meet these challenges, we model battery output voltage dynamics adaptively.

Fig. 5 depicts our CPS-perspective approach. Instead of using a pre-defined model, we first build a generic model form that captures the battery behaviors related to measurable physical quantities. To adaptively construct its generic model

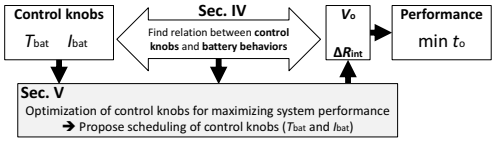

Fig. 5. Approach overview: Section IV describes how to refine a battery behavior model, and Section V propose how to determine control knobs (I_{bat} and T_{bat}) to maximize the performance based on the refined battery behavior model.

form, we employ an efficient regression scheme utilizing experimental data to distill online physical parameters that affect the battery behavior significantly. The generic model is then "customized" for each battery pack because each pack in different vehicles has different characteristics. By using the model constructed above, we solve the problems and choose efficient control knobs while considering its performance. Finally, we propose a real-time scheduling policy that determines the discharge-rate and temperature of battery via an analysis of the solution.

IV. Construction of Models for Battery Prognosis

As discussed in Section III-B, we should characterize the impact of the control knobs on battery behaviors ($V_{\text{o}}, R_{\text{int}}$) and system performance ($min\{t_{\text{o}}\}$). To this end, we first explore measurable physical quantities that impact the system performance, and then describe how to extract effective physical quantities and/or their combinations. Finally, we construct battery behavior models based on these effective physical quantities for prognosis of batteries as shown in Fig. 6.

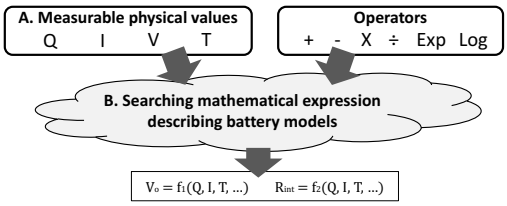

Fig. 6. Building battery behavior models (output voltage and degradation model) for prognosis of batteries

A. Candidate physical quantities

Operation-time is the most important performance metric as it represents how long batteries can supply the required power, while *degradation rate* captures how quickly the operation-time deteriorates. So, we should figure out physical quantities affecting the battery behaviors and performance (operation-time and degradation rate) to prognose the batteries. Based on existing studies, we have identified candidate physical quantities affecting the battery operation-time and degradation as summarized in Table I.

1) Physical quantities affecting operation-time: We identified three physical quantities that greatly affect battery operation-times: battery discharge/charge current ($I_{\text{bat}}(t)$), the amount of discharges ($Q_{\text{d}}(t)$), and battery temperature ($T_{\text{bat}}(t)$).

The discharge/charge current ($I_{\text{bat}}(t)$) is the most important physical quantity influencing the system performance in various ways [2, 20, 21]. A high discharge current reduces battery

System performance	Physical quantity	Description
Operation-time (t_o)	$I_{bat}(t)$	Battery discharge/charge current
	$\frac{dI_{bat}}{dt}(t)$	The rate change of battery discharge/charge current
	$\frac{dV_{bat}}{dt}(t)$	The rate change of battery voltage
	$Q_d(t) = \int_0^t I_{bat}(\tau)d\tau$	The amount of discharged charge
	$T_{bat}(t)$	Battery temperature
Degradation rate at k^{th} cycle (ΔR_{int}^k)	$\frac{1}{t_o^k}\int_0^{t_o^k} \lvert I_{bat}(t)\rvert dt$	The average amount of battery discharge/charge current
	$Q_d^k = \int_0^{t_o^k} I_{bat}(t)dt$	The amount of discharged charge
	$\int_0^{t_o^k} T_{bat}(t)dt$	Accumulative temperature exposure

TABLE I. PHYSICAL QUANTITIES AFFECTING SYSTEM PERFORMANCE (OPERATION-TIME (t_O) AND BATTERY DEGRADATION (ΔR_{INT}))

operation-time because such a high discharge current causes its output voltage to drop, and the battery to provide less energy than the battery with a lower discharge current, called the *rate-capacity* effect. On the other hand, during periods of low or no discharge current, the battery voltage can recover to a certain extent, which is termed the *recovery* effect. For instance, a high load causes a temporary voltage drop, and then a part of the cell voltage is recovered after a certain period of rest as shown in Fig. 7. The figure also shows that battery output voltage is dependent on the remaining charge in the battery, or *State-of-Charge* (SoC) $= 1 - \frac{Q_d(t)}{Q_{max}}$ [22]. Note that we can estimate the SoC based on the amount of discharge current ($Q_d(t) = \int_0^t I_{bat}(\tau)d\tau$). Meanwhile, battery temperature ($T_{bat}(t)$) affects its operation-time. A higher temperature stimulates the mobility of electron or ion, temporarily increasing its capacity [23] with a reduced internal resistance.

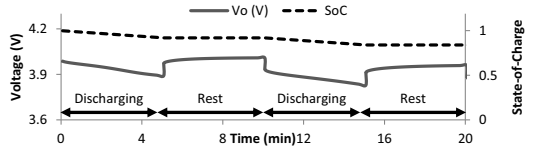

Fig. 7. The output voltage (V_{bat}) and state-of-charge (SoC) when a battery is discharged at 23 A/m^2 of current and rested at 0 A/m^2 repeatedly. The results are extracted from evaluation tools/settings to be described in Section VI.

2) Physical quantities affecting battery degradation: During the warranty period, the operation-time keeps on decreasing due to battery degradation (ΔR_{int}), and depends on the average amount of discharge/charge current ($\frac{1}{t_o^k}\int_0^{t_o^k} |I_{bat}(t)|dt$), the amount of emitted charges (Q_d^k), and cumulative temperature exposure ($\int_0^{t_o^k} T_{bat}(t)dt$) at the k^{th} cycle as shown in Table I. The average charge/discharge current ($\frac{1}{t_o}\int_0^{t_o} |I_{bat}|dt$) affects the degradation rate of a battery. The battery degradation is known to accelerate exponentially with an increase of the discharge current density [24]. Also, performance degradation rate is closely related to how much energy is discharged in a cycle (Depth-of-Discharge, DoD) [25], which can be measured by SoC ($|SoC|_{t=t_o}$) at the end of the cycle. On the other hand, the cumulative temperature exposure ($\int_0^{t_o} T_{bat}dt$) affects the degradation rate as explained next. The level of battery performance degradation depends on the time and thermal stresses to which the battery has been exposed, and it can be represented by a rise of battery internal resistance [26].

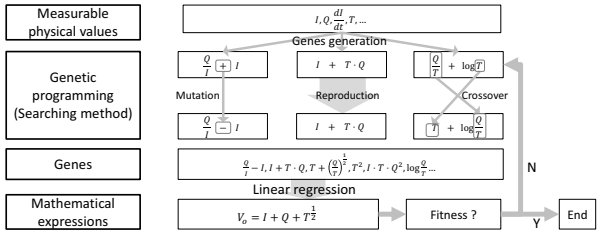

Step 1 : Generate random genes;
Step 2 : Generate genes for next generation via reproduction, mutation, and crossover of parent genes;
Step 3 : Execute ordinary least squares to regression to find weights of genes;
Step 4 : Check its fitness and jump to Step 2 if the fitness is not satisfied.

Fig. 8. Symbolic regression process

B. Construction of a battery behavior model via symbolic regression with genetic programming

We have investigated physical quantities affecting battery output voltage and degradation. Here we discuss a systematic way to extract physical quantities and construct battery behavior models describing how they affect the output voltage and the rate of degradation from data. We first introduce symbolic regression with genetic programming for constructing battery behavior models. Then, we present the process of building a battery behavior model via the symbolic regression while addressing the issues in exploiting the regression scheme.

1) Symbolic regression with genetic programming: Symbolic regression is a type of regression analysis. This regression searches the space of mathematical expressions to find the model that best fits a given data set, both in terms of accuracy and simplicity [27, 28]. Unlike traditional linear and nonlinear regression methods that fit parameters to an equation of a given form, symbolic regression searches both parameters and form of equations simultaneously. Searching for effective genes is done by *genetic programming*, which is an evolutionary algorithm-based method (inspired by biological evolution) to find the best mathematical expression as shown in Fig. 8 [29]. The symbolic regression with genetic programming has already been substantiated as its effectiveness for automated processes distilling the data into natural law model in the form of analytic mathematical expression [30]. Therefore, we exploit this regression scheme to construct accurate battery models, because chemical reactions occurring in batteries follow physical laws.

2) Battery behavior model construction process: Fig. 8 shows an example of the symbolic regression process to generate the battery behavior model. For the first generation, we generated genes ($\frac{Q}{I} + I$, $I + T \cdot Q$, $\frac{Q}{T} + \log T$) in a random way based on measurable physical quantities and mathematical operations. Then, we constructed the first battery behavior model consisting of the random genes with their weights. The model is tested in terms of its fitness, and then, if the fitness is not satisfied, we should explore other models to find a better one in a search space. In such a case, we generate genes for the next generation via a *mutation* ($\frac{Q}{I} + I \rightarrow \frac{Q}{I} - I$) and a *crossover* ($\frac{Q}{T} + \log T \rightarrow T + \log \frac{Q}{T}$) based on the parents' genes that have low weights. We execute a *reproduction* ($I + T \cdot Q$) of genes with large weights to leave the genes that are likely to

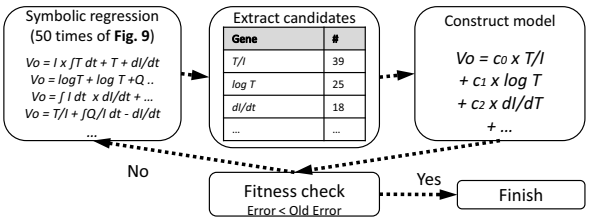

Step 1 : Execute symbolic regression 50 times and store the generated genes from the regression;

Step 2 : Sort the generated genes in order of occurrence and select genes that frequently occurs;

Step 3 : Construct generic behavior models based on the selected genes;

Step 4 : Check its fitness.

Fig. 9. Algorithm for constructing a battery behavior model

critically affect the model. We check its fitness and repeatedly generate new generations until the fitness is satisfied.

In applications exploiting the symbolic regression, the identification of nontrivial relations is a major challenge. For example, $x^{\frac{1}{100}}$ can be selected for the gene because it may improve its fitness even if it would not affect the results much. Our key insight into identifying nontrivial genes is that nontrivial genes would appear more than trivial genes. To find the most effective nontrivial genes for modeling battery behavior, we iterate the symbolic regression many times. Then, we sort the genes in the order of occurrence, and select the frequently appeared genes. For instance, at step 1, we executed 50 symbolic regressions and stored the generated genes. We select $\frac{dI}{dt}$, $\frac{T}{I}$, log T and so on, because it was generated frequently and thus likely to be nontrivial genes. Based on the extracted nontrivial genes, we construct the battery behavior model and repeat this process until the fitness is good enough to use them. Fig. 9 shows the entire process for constructing a battery behavior model.

V. Scheduling of Battery Temperature and Discharge/Charge Current

So far, we have abstracted battery behaviors affecting its operation-time and degradation rate. We now use this abstraction to systematically schedule the control knobs for solving the problem described in Section III-A. Before presenting a scheduling policy, we first determine the relationship between performance metrics (t_{o} and ΔR_{int}) and control knobs (I_{bat} and T_{bat}) to get an insight into efficient schedulings of the control knobs.

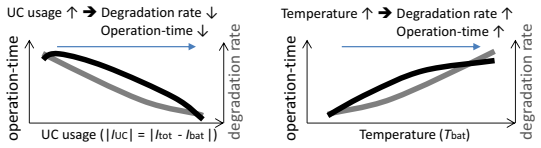

Fig. 10. The effects of the thermal and discharge-rate control on the system performance.

A. Relationship between operation-time and degradation rate

Battery operation-time, degradation rate, and control knobs are all closely related to each other. For example, old batteries whose internal resistances are high, cannot operate longer to power EVs than new batteries, recorded as follows:

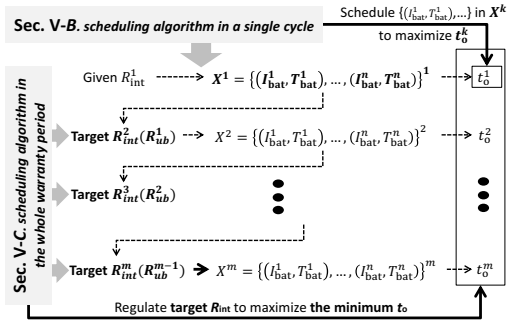

Fig. 11. The entire scheduling process. Section V-B presents an algorithm determining a control knob vector (X^{k}) for maximizing the operation-time (t_{o}^k) in a single cycle. Section V-C provides an algorithm of searching for the target degradation levels (R_{ub}) of each cycle for maximizing the minimum operation-time ($min\{t_{\mathrm{o}}^1, \ldots, t_{\mathrm{o}}^m\}$).

- $R_{\mathrm{int}}^i \uparrow (\downarrow) \Longrightarrow t_{\mathrm{o}}^i \downarrow (\uparrow)$.

Also, the degradation rate depends on how the battery is used. Fig. 10 presents a general trend of operation-time and degradation rate related to the temperature and discharge/charge current. For instance, excessive use of UCs degrades its effectiveness because storing/extracting charge to/from UCs causes additional energy dissipation due to their internal resistance. In contrast, increasing use of UCs decelerates battery degradation since it can reduce battery discharge/recharge stress. Meanwhile, high temperature increases battery capacity by reducing battery internal resistance during an operation cycle. Unfortunately, continuous/frequent exposure to high temperature accelerates battery degradations. In summary, the following relation holds:

- $t_{\mathrm{o}}^i \downarrow (\uparrow) \Longleftrightarrow \Delta R_{\mathrm{int}}^i \downarrow (\uparrow)$.

These trends are used to maximize the minimum operation-time during the warranty period. Basically, we use a different control policy for a different cycle during the warranty period. For example, during very early cycles, we increase use of UCs at low temperature for future use of battery. In contrast, during late cycles of the warranty period, we focus only on its operation-time, rather than the degradation rate, because we do not have to consider the degradation level after the warranty period.

B. Scheduling algorithm in a single operation cycle

Fig. 11 shows the entire process of determining the control knob matrix X. We first represent a scheduling policy to maximize operation-time (t_{o}) for the target degradation level (R_{int}) in a single cycle. Note that the target degradation level (R_{int}^{k+1}) is key in regulating the operation-time (t_{o}) of each cycle so as to maximize the minimum operation-time. Section V-C details how to determine the target degradation levels (R_{int}^{k+1}) to maximize the minimum operation-time during the entire warranty cycle.

1) Scheduling requirement in one operation cycle: To maximize the operation-time in a cycle, we should maximize the time duration during which battery output voltage is within an applicable range for motors' operation while supplying the required energy. In the example in Fig. 12(a), the battery cannot supply the required power with an applicable voltage after initial t_{o}, the operation-time of this scheduling, potentially

Algorithm 1 Algorithm for optimization in a cycle

1: **procedure** PROC1($R_{\rm ub}$,$R_{\rm int}$,$P_{\rm req}$)
2: $X_{\rm k} \leftarrow X_{\rm k}$ that has no additional power for the auxiliary devices;
3: /* Reduce $\Delta R_{\rm int}$ via $X_{\rm k}$ control if it is larger than the target $\Delta R_{\rm int}$ */
4: **while** $R_{\rm ub} < R_{\rm int}$ **do**
5: Set a target accumulative physical quantities that reduce $\Delta R_{\rm int}$
6: **end while**
7: $X_{\rm k} \leftarrow$ Search $X_{\rm k}$ maximizing $t_{\rm o}$ at $P_{\rm req}$ and maintaining the target cumulative physical quantities via the discharge current and temperature scheduling (Supplement file)
8: /* We can estimate $t_{\rm o}$ and $\Delta R_{\rm int}$ at X^k for supplying $P_{\rm req}$ via the behavior models constructed in Section IV*/
9: **return** $[t_{\rm o}, R_{\rm int}, X_{\rm k}]$;
10: **end procedure**

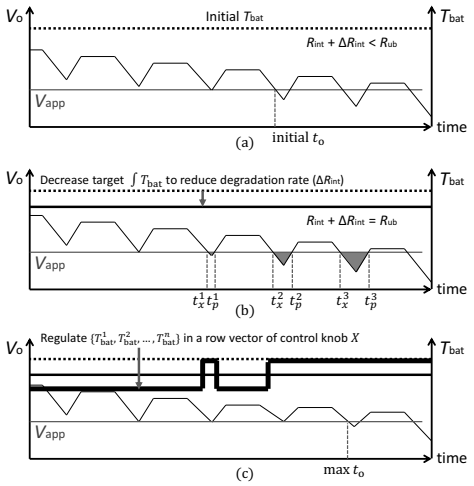

Fig. 12. An example of the temperature scheduling in a cycle

stopping the motor operation. To increase operation-time, we have to compensate the voltage shortage by relieving the discharging stress or helping chemical reactions in the battery via discharge current and/or temperature control. In the meantime, we have to maintain the battery degradation level ($R_{\rm int}$) within the required range ($< R_{\rm ub}$) for its future usability. The next subsection provides a detailed algorithm for extending operation-time while keeping the degradation rate below the specified level.

2) Algorithm for a single cycle: Algorithm 1 describes how to determine vectors of ($I^i_{\rm bat}$, $T^i_{\rm bat}$) in a single cycle. Initially, the minimum use of the thermal fins or energy buffers is set (Line 2). It would not be the best solution because the required degradation rate may not be satisfied and/or the output voltage of battery could be dropped quickly as shown in Fig. 12 (a). First, to meet the required degradation rate at the $k^{\rm th}$ cycle, steps (Line 4–6, Fig. 12 (b)) determine the target cumulative physical quantities affecting the degradation described in Table I. The final step (Line 7, Fig. 12 (c)) determines a pair of ($I^i_{\rm bat}$, $T^i_{\rm bat}$) of each control interval to compensate as many voltage drop periods as possible while maintaining the required cumulative physical quantities. A detailed algorithm for Line 7 is presented in the supplementary file [19].

Algorithm 2 Algorithm for optimization within a whole period

1: **procedure** PROC2($N_{\rm w}$, $R_{\rm ub}$, $R^1_{\rm int}$, $P_{\rm req}$)
2: $[t^1_{\rm o}, R^2_{\rm int}, X^1] \leftarrow$ PROC1(∞, $R^1_{\rm int}$, $P_{\rm req}$);
3: **for** $i = 2; i \leq N_{\rm w}; i$++ **do**
4: $[t^i_{\rm o}, R^{i+1}_{\rm int}, X^i] \leftarrow$ PROC1(∞, $R^i_{\rm int}$, $P_{\rm req}$);
5: $R^{i-1}_{\rm UB} \leftarrow R^i_{\rm int}$
6: **while** $t^i_{\rm o} \neq t^{i-1}_{\rm o}$ **do**
7: // To increase $t_{\rm o}$, decrease $R_{\rm int}$
8: $R^{i-1}_{\rm ub} \leftarrow R^{i-1}_{\rm ub} - 0.01$;
9: $[t^{i-1}_{\rm o}, R^i_{\rm int}, X^{i-1}] \leftarrow$ PROC1($R^{i-1}_{\rm ub}$, $R^{i-1}_{\rm int}$, $P_{\rm req}$);
10: $[t^i_{\rm o}, R^{i+1}_{\rm int}, X^i] \leftarrow$ PROC1($R^i_{\rm ub}$, $R^i_{\rm int}$, $P_{\rm req}$);
11: **end while**
12: **end for**
13: **return** $[t_{\rm o}, X]$;
14: **end procedure**

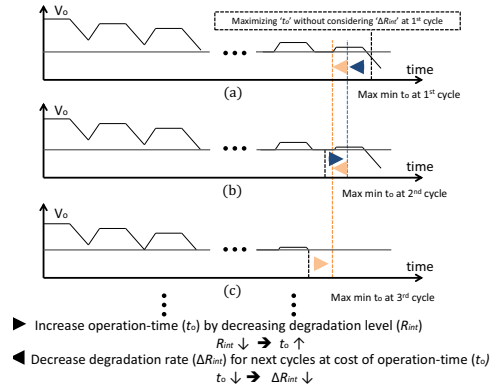

Fig. 13. Determination of each target $R_{\rm int}$ to maximize the minimum operation-time

C. Scheduling algorithm during the whole warranty period

So far, we proposed a scheduling algorithm for maximizing operation-time in a cycle while satisfying the required degradation rate ($\Delta R_{\rm int}$). We now expand the algorithm for the whole warranty period to maximize the minimum operation-time (min $\{t_{\rm o}\}$) based on the impact of battery thermal and discharge-rate control on the operation-time and degradation rate.

1) Optimization within warranty period: Algorithm 2 determines the target degradation rate ($R_{\rm ub}$) for each cycle to maximize the minimum operation-time. At the first step (Line 2), the temperature and discharge current are scheduled without considering the battery degradation rate as shown in Fig. 13 (a). The battery temperature would be set only for its safety, and therefore UCs are used as little as possible to save additional energy consumption by the auxiliary devices. Next, the target degradation level is regulated for the present cycle (Line 8) to increase the operation-time during the next cycle. Even if it may cause inefficiency in terms of the operation-time of the present cycle, we can improve the overall system performance by increasing the worst-case operation-time during the warranty period. We iterate this process until all the operation-times become similar as shown in Figs. 13 (b) and (c).

D. Real-time scheduling algorithm

To schedule the temperature and discharge current needed to achieve our goal, we first solve the scheduling problem

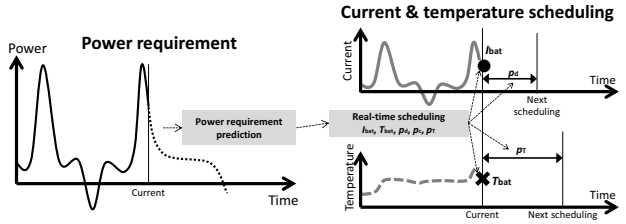

Fig. 14. Real-time prediction and scheduling for battery discharge current and temperature

for a given power requirement. Typically, the future power requirement is unknown, because it depends on a number of variables, including, but not limited to, driving conditions, vehicle type, and road conditions. But, solving for a given power requirement allows for the creation of an implementable schedule. Using past power requirement patterns, we can determine the amount of power needed for a few seconds of battery usage [10]. Based on these patterns, we can adopt a power requirement predictor and determine the discharge current and temperature in real time based on the prediction as shown in Fig. 14. We should also determine the frequency at which discharge current and temperature must be determined (scheduling period). This scheduling period is used to preclude batteries from inefficient usage.

Algorithm 3 Algorithm for real-time discharge current scheduling

```
1: procedure PROC3(I_tot, I*_bat)
2:     while Driving do
3:         if Recharge then
4:             I_bat = 0;
5:             Sleep(p_c);
6:         else if I_bat < I*_bat then
7:             I_bat = I_tot;
8:         else
9:             I_bat = I*_bat;
10:            Sleep(p_d);
11:        end if
12:    end while
13: end procedure
```

The scheduling results shown in Fig. 18 give insight into the real-time scheduling of the discharge current. The UCs should be fully recharged when the braking system generates energy. They can then supply some of the stored charge to the motor, based on the target degradation rate. Algorithm 3 schedules discharge current in real time. It requires both the present total discharge current (I_{tot}) and the target battery discharge current (I^*_{bat}) needed to control the degradation rate. First, when the power is recharged from the braking system, the battery current is set to 0 to charge the UC. Then, the discharge current is rescheduled after p_{c}. If the battery is discharged to the electric load, the target battery discharge current is determined based on its amount. If it is in the normal discharge range ($I_{\text{bat}} < I^*_{\text{bat}}$), the battery is allowed to supply charges to the load ($I_{\text{bat}} = I_{\text{tot}}$). If it is outside of the normal range, the UC provides charges to maintain the battery discharge current ($I_{\text{bat}} = I^*_{\text{bat}}$). Later, the discharge current is scheduled (p_{d}). The scheduling period (p_{d} and p_{c}) must be determined carefully for real-time scheduling. Otherwise, it may lead to additional power consumption. For instance, if the discharge current is not rescheduled in time, the battery discharges energy to the UC, even though the UC does not require power. From the power requirement prediction, the length of the discharge/charge period can be estimated (p^*_{d} / p^*_{c}). We set p_{d} (p_{c}) to p^*_{d} (p^*_{c}) over 10. Real-time temperature scheduling is similar to the discharge current scheduling, and thus we omitted the result.

VI. Evaluation

We now evaluate the proposed battery model construction and scheduling of battery temperature and discharge/charge current. We first describe tools and setups for the evaluation, and then demonstrate the accuracy of battery behavior predictions and performance improvement by our scheduling system.

A. Evaluation settings

To test the proposed model construction, we exploit real data including battery discharge/charge current (I_{bat}), temperature (T_{bat}), and output voltage (V_{o}) by using Neware's battery tester [31]. We measure the performance improvement of the proposed temperature and current scheduling by using commonly-used vehicle (*Advisor 2.0*) [32] and battery simulator (*Dualfoil5*) [33]. To make the simulation more realistic, we obtained real driving data from "The US Environmental Protection Agency (EPA)" and "California Air Resources Board" such as ARB02, SC03 and LA92.

B. Evaluation results

Our goal is to maximize the minimum battery operation-time during the warranty period by determining efficient battery temperature and discharge/charge current. For effective temperature and current schedules, we constructed a battery behavior model. We evaluate the following schemes for modeling battery voltage and degradation rate:

- V-LR: battery voltage model via linear regression with a circuit-based battery model;
- V-SVR: battery voltage model via support vector regression;
- V-SR: our battery voltage model via symbolic regression described in Section IV;
- R-LR : battery degradation rate model via linear regression with temperature (*likewise* discharge current) linear degradation model;
- R-SVR : battery degradation rate model via support vector regression;
- R-SR: battery degradation rate model via symbolic regression with described in Section IV.

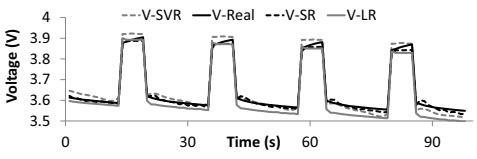

Fig. 15. An example of battery output voltage predictions.

Table II shows the error of the constructed model of V-SR, V-SVR and V-LR for battery output voltage prediction, and Fig. 15 plots their predictions. Root-mean-square error (RMSE) is used to measure the prediction accuracy. As shown

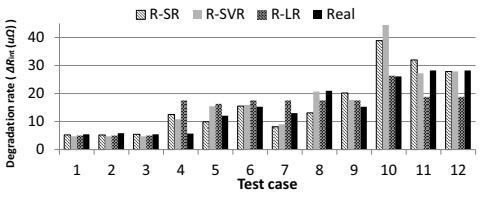

Fig. 16. Degradation rate predictions. We use 12 degradation patterns from the battery tester. We select 10 degradation patterns to build a degradation model and validate the model with 2 remaining degradation cases. The validation process is then repeated 6 times (6-fold cross-validation).

in this table, V-SR improves the accuracy of the model by up to 67.9% (49.8%), compared to V-LR (V-SVR). The basis form of V-LR is a circuit-based battery model whose internal resistance depends on temperature exponentially [5]. However, at low temperature, the accuracy of the model is lower than that of V-SR, because the exponential internal resistance model is correct only for a specific range of temperature. So, while V-SVR predicts the output voltage more accurately than V-LR, V-SR has the best overall prediction accuracy of the three output voltage models. Table III and Fig. 16 show the errors of degradation predictions. R-SR shows improvements of prediction accuracy by 5.6% and 8.0% over R-LR and R-SVR, respectively. That is, the degradation rate model constructed based on various physical quantities yields an accurate behavior model to predict the battery's states.

Prediction methods	prediction error $E(V_o)$
V-LR	0.00336
V-SVR	0.00215
V-SR	0.00108

TABLE II. AVERAGE ERROR OF BATTERY OUTPUT VOLTAGE PREDICTION

Prediction methods	prediction error E(R_{int})
R-LR	1.626
R-SVR	1.668
R-SR	1.535

TABLE III. AVERAGE ERROR OF BATTERY DEGRADATION PREDICTION (R_{int})

1) Performance of the proposed scheduling policy: We have evaluated the following three discharge/charge current and temperature scheduling schemes:

- Const-TI: fixed operational temperature and discharge-rate;
- Opt-TI: our scheduling scheme described in Section IV;
- RT-TI: our real-time scheduling scheme described in Section IV.

	Minimum operation-time (t_o) (s)		
Prediction methods	ARB02	LA92	SC03
Const-TI	407	331	321
Opt-TI	451	396	595
RT-TI	407	368	554

TABLE IV. MINIMUM OPERATION-TIMES

We ran simulation and extracted operation-times during the warranty period of each scheme under various electric loads. The minimum operation-times are then extracted to evaluate the schemes. As shown in Table IV, Opt-TI improves the minimum operation-time by up to 10.8% at ARB02,

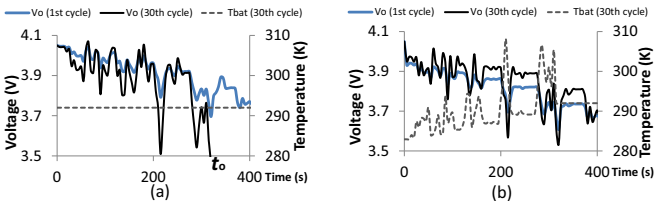

Fig. 17. Voltage profiles during the first cycle and the last cycle (30) for SC03 driving under Opt-TI scheduling. Compared to Const-TI, the voltage drop was tolerable due to pre-heating the battery and lower degradation level.

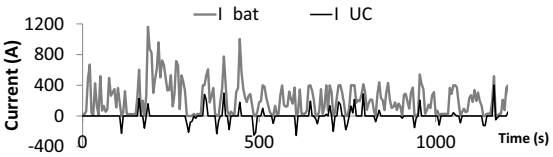

Fig. 18. UC current (I_{UC}) profile for SC03 under Opt-TI. I_{UC} helps the battery when it is required to supply high power by mitigating the discharge/charge stress to the battery.

19.6% at LA92 and 85.3% at SC03, respectively, over Const-TI. Figs. 17 (a) and 18 present examples of battery voltage and scheduled temperature (T_{bat}) and battery discharge/charge current (I_{bat}) under Opt-TI during the first and the last cycles. The algorithm pre-heats batteries and pre-charges UCs to preclude the batteries from a fast voltage drop. By comparing Figs. 17 (a) and (b), we can see the differences between Const-TI and Opt-TI during early cycles and late cycles. As we discussed in Section V-C, Opt-TI utilizes the thermal and discharge/charge current management much at early cycles to decelerate the battery degradation. Then, it maximizes operation-time without considering its degradation during late cycles. Therefore, although battery output voltage during early cycles of Opt-TI (in Fig. 17 (b)) is lower than that of Const-TI (in Fig. 17 (a)), Opt-TI could maintain the output voltage within the applicable range longer than Const-TI during the last cycle, because Opt-TI decelerated the battery degradation during early cycles. The battery behavior models constructed in Section IV enable our BMS to determine a pair of (I_{bat}, T_{bat}) at each control interval under Opt-TI, because they allow the BMS to predict battery operation-time and degradation rate with respect to (I_{bat}, T_{bat}) schedules. The derived real-time prediction model, RT-TI, determines the temperature and discharge current of a given cycle, while the target degradation rate is calculated by the model Opt-TI. The simulation shows that the minimum battery operation-time of RT-TI is generally similar to the LA92 and SC03 cases of the Opt-TI model. However, certain conditions, like highly variable driving patterns in one case (ARB02), reduced the operation-time of the RT-TI model. In extreme cases, like ARB02, the minimum battery operation-time is similar to the Const-TI.

VII. CONCLUSION

In this paper, we have proposed a new integrated BMS that schedules the amount of energy pre-charged into UCs and battery temperature at each control interval based on the analysis of their impact on the battery capacity and degradation. We have also proposed a battery prognosis scheme, which is able to predict when the battery cannot provide the required power. Our evaluation with real battery data and realistic driving simulation shows that the proposed schemes make a significant

improvement in BMS's efficiency over a simple method used in the existing BMSes for EVs.

In future we would like to improve the BMS using the proposed architecture. Primarily, the accuracy of the prognosis scheme and power requirement predictions should be enhanced for efficient discharge/charge current and temperature schedule. This could be achieved by increasing the accuracy of the battery behavior and power requirement models. For this, we have to process the model construction after acquiring lots of battery behavior and driving data under various conditions via a remote prognosis system. Our framework can also be used for other types of batteries including fuel cells which have their own power and energy densities, because battery behavior models are extracted by using behavior data of the batteries installed in the system, and scheduling discharge/charge current and temperature of the batteries based on the constructed behavior model.

ACKNOWLEDGMENTS

The work reported in this paper was supported in part by (i) the NSF under grants CNS-1446117 and CNS-1329702; (ii) LG Chem Ltd.; (iii) the DGIST R&D Program of MSIP of Korea (CPS Global Center) and the Global Research Laboratory Program through NRF funded by MSIP of Korea (2013K1A1A2A02078326); (iv) Basic Science Research Program through NRF funded by MSIP of Korea (NRF-2014R1A1A1035827).

REFERENCES

[1] J. TROP and D. CARDWELL, "Tesla plans 5 billion battery factory for mass-market electric car," Feb 2014. [Online]. Available: http://www.nytimes.com/2014/02/27/automobiles/tesla-plans-5-billion-battery-factory-for-mass-market-electric-car.html?_r=0

[2] H. Kim and K. G. Shin, "Scheduling of battery charge, discharge, and rest," in *Proceedings of the 30th IEEE Real-Time Systems Symposium (RTSS)*, 2009, pp. 13–22.

[3] E. Kim, K. Shin, and J. Lee, "Real-time discharge/charge rate management for hybrid energy storage in electric vehicles," in *Real-Time Systems Symposium (RTSS), 2014 IEEE*, Dec 2014, pp. 228–237.

[4] L. He, L. Gu, L. Kong, Y. Gu, C. Liu, and T. He, "Exploring adaptive reconfiguration to optimize energy efficiency in large-scale battery systems," in *Real-Time Systems Symposium (RTSS), 2013 IEEE 34th*, Dec 2013, pp. 118–127.

[5] E. Kim, J. Lee, and K. G. Shin, "Real-time battery thermal management for electric vehicles," in *ACM/IEEE 5th International Conference on Cyber-Physical Systems*, Berlin, Germany, Apr 2014.

[6] G. Motors. (2009) The chevrolet volt cooling/heating systems explained. [Online]. Available: http://gm-volt.com/2010/12/09/the-chevrolet-volt-coolingheating-systems-explained/

[7] F. M. Company. (2013) Ford uses innovative liquid-cooled battery system to help focus electric owners maximize range. [Online]. Available: http://media.ford.com/article_display.cfm?article_id=33185

[8] R. Smith, S. Shahidinejad, D. Blair, and E. Bibeau, "Characterization of urban commuter driving profiles to optimize battery size in light-duty plug-in electric vehicles," *Transportation Research Part D: Transport and Environment*, vol. 16, no. 3, pp. 218 – 224, 2011.

[9] T.-K. Lee, B. Adornato, and Z. Filipi, "Synthesis of real-world driving cycles and their use for estimating phev energy consumption and charging opportunities: Case study for midwest/u.s." *Vehicular Technology, IEEE Transactions on*, vol. 60, no. 9, pp. 4153–4163, 2011.

[10] E. Kim, J. Lee, and K. G. Shin, "Real-time prediction of battery power requirements for electric vehicles," in *ACM/IEEE 4th International Conference on Cyber-Physical Systems*, Philadelphia, PA, Apr 2013.

[11] C. Lv, J. Zhang, Y. Li, and Y. Yuan, "Regenerative braking control algorithm for an electrified vehicle equipped with a by-wire brake system." SAE International, 04 2014.

[12] Y. Gao, L. Chen, and M. Ehsani, "Investigation of the effectiveness of regenerative braking for ev and hev." SAE International, 08 1999.

[13] Y. Gao and M. Ehsani, "Electronic braking system of ev and hev—integration of regenerative braking, automatic braking force control and abs." SAE International, 08 2001.

[14] S. Pay and Y. Baghzouz, "Effectiveness of battery-supercapacitor combination in electric vehicles," in *Power Tech Conference Proceedings, 2003 IEEE Bologna*, vol. 3, June 2003, pp. 6 pp. Vol.3–.

[15] Y. Kim, S. Park, Y. Wang, Q. Xie, N. Chang, M. Poncino, and M. Pedram, "Balanced reconfiguration of storage banks in a hybrid electrical energy storage system," in *Computer-Aided Design (ICCAD), 2011 IEEE/ACM International Conference on*, Nov 2011, pp. 624–631.

[16] J. Cao and A. Emadi, "A new battery/ultracapacitor hybrid energy storage system for electric, hybrid, and plug-in hybrid electric vehicles," *Power Electronics, IEEE Transactions on*, vol. 27, no. 1, pp. 122–132, Jan 2012.

[17] A. Pesaran, S. Burch, and M. Keyser, "An approach for designing thermal management systems for electric and hybrid vehicle battery packs," London, UK, May 1999.

[18] G.-H. Kim and A. Pesaran, "Battery thermal management system design modeling," Yokohama, Japan, Oct 2006.

[19] E. Kim. (2015) Supplement: Modeling and real-time scheduling of large-scale batteries for maximizing performance. [Online]. Available: https://kabru.eecs.umich.edu/?page_id=4

[20] L. Benini, A. Macii, E. Macii, M. Poncino, and R. Scarsi, "Scheduling battery usage in mobile systems," *IEEE Transactions on VLSI systems*, vol. 11, no. 6, pp. 1136–1143, 2003.

[21] "Factors that affect cycle-life and possible degradation mechanisms of a li-ion cell based on licoo2," *Journal of Power Sources*, vol. 111, no. 1, pp. 130 – 136, 2002.

[22] "State-of-charge and capacity estimation of lithium-ion battery using a new open-circuit voltage versus state-of-charge," *Journal of Power Sources*, vol. 185, no. 2, pp. 1367 – 1373, 2008.

[23] C. Park and A. Jaura, "Dynamic thermal model of li-ion battery for predictive behavior in hybrid and fuel cell vehicles," in *SAE Technical Paper 2003-01-2286*, 2003.

[24] "Development of long life lithium ion battery for power storage," *Journal of Power Sources*, vol. 101, no. 1, pp. 53 – 59, 2001.

[25] G. Ning and B. N. Popov, "Cycle life modeling of lithium-ion batteries," vol. 151, no. 10, pp. A1584–A1591, 2004.

[26] E. Thomas, I. Bloom, J. Christophersen, and V. Battaglia, "Rate-based degradation modeling of lithium-ion cells," *Journal of Power Sources*, vol. 206, no. 0, pp. 378 – 382, 2012.

[27] D. P. Searson, D. E. Leahy, and M. J. Willis, "Gptips: an open source genetic programming toolbox for multigene symbolic regression," in *Proceedings of the International multiconference of engineers and computer scientists*, vol. 1. Citeseer, 2010, pp. 77–80.

[28] D. A. Augusto and H. J. Barbosa, "Symbolic regression via genetic programming," in *Neural Networks, 2000. Proceedings. Sixth Brazilian Symposium on*. IEEE, 2000, pp. 173–178.

[29] J. R. Koza, *Genetic programming: on the programming of computers by means of natural selection*. MIT press, 1992, vol. 1.

[30] M. Schmidt and H. Lipson, "Distilling free-form natural laws from experimental data," vol. 324, no. 5923, pp. 81–85, 2009.

[31] Neware. Battery tester. http://www.newarebattery.com/.

[32] NREL. Advisor 2002. http://www.nrel.gov/.

[33] M. Doyle and J. Newman. Dualfoil5. [Online]. Available: http://www.cchem.berkeley.edu/jsngrp/fortran.html